Current Collection to Long, Thin Probes in a Dense High-Speed Flowing Plasma

Brian E. Gilchrist[1], Sven G. Bilén[2], and Alec D. Gallimore[1]

[1] *University of Michigan, Ann Arbor, Michigan 48109*
[2] *The Pennsylvania State University, University Park, Pennsylvania 16802*
(734) 763–6230, gilchrst@umich.edu

Abstract. We describe chamber tests of simulated electrodynamic tethers (EDTs) of different geometries operating in a dense, high-speed plasma. The geometries tested were cylindrical, flat-ribbon, and sparse-ribbon or mesh. Several important conclusions that can be drawn from the tests are as follows: the currents collected by cylinder are close to what would be predicted via orbital-motion-limited (OML) current collection theory. The tape tether had comparable current levels to a theoretical equal area OML cylinder collector. However, I–V behavior clearly is different at nearest distances ($\sim 15\ \lambda_D$ tape width) as compared to furthest test distances ($\sim 6\ \lambda_D$ tape width). The tape tether did better than a theoretical equal mass solid cylinder. A "knee" in the I–V curves can be seen in the tape/mesh data at a potential that is just above the estimated energy of the incoming beam of ions, at least for the closest distances where Debye length is smallest. Below this knee the current increases rapidly as voltage is increased. Above the knee the current increases at a rate one might expect from OML current-collection models depending on the relative width. This likely is an example of high-speed plasma flow effect. Perpendicular tape orientation performed slightly better than parallel.

INTRODUCTION

It has been proposed that operating in the orbital-motion-limited (OML) regime is especially beneficial for electron current collection to thin, bare electrodynamic tethers (EDTs) with width dimensions on the order of a Debye length (Sanmartín et al., 1993). This configuration is different than that of Tethered Satellite System missions (TSS–1 and –1R), which used a large (with respect to λ_D spherical collector for electron collection. It is predicted theoretically that a bare tether will be a highly efficient collector of ionospheric electrons (per unit area) when compared to other current collection geometries at equal bias (such as TSS) and it also has been suggested that a combination of technologies may be useful.

As part of NASA's Advanced Space Transportation Program, the Propulsive Small Expendable Deployer System (ProSEDS) mission (Johnson et al., 1998), which is to fly in early 2001, will be the first to use the bare-tether concept and will demonstrate high current and measurable thrust; the technology is also being considered for other future missions. However, a small, thin cylinder is not necessarily the best tether design when considering other practical factors such as tether lifetime. For example, to increase tether lifetime, a tether based on ribbon-like geometry (*e.g.*, flat and wide) or more sparse structures of equal series resistance may be preferred; hence, these tethers would have dimensions exceeding a Debye length. These new geometries pose several questions that must be addressed before they can be employed. For example, how will the current collection performance change as a function of geometry and Debye length when in an ionospheric plasma at orbital velocities? Does the orientation of the ribbon with respect to the flowing plasma direction have an impact on collection efficiency?

This work describes two sets of vacuum chamber tests that simulated EDTs of different geometries operating in a dense, high-speed plasma. The geometries described here were cylindrical and flat-ribbon tape. The cylinder sample had a radius ranging 1–3 Debye lengths (as plasma parameters were varied) whereas the tape had a width that ranged from 5–19 Debye lengths. For these tests, the 6-m × 9-m chamber operated by Michigan's Plasmadynamics and Electric Propulsion Laboratory (PEPL) was used along with a PEPL/USAF-designed Hall thruster for the plasma

CP552, *Space Technology and Applications International Forum–2001*, edited by M. S. El-Genk

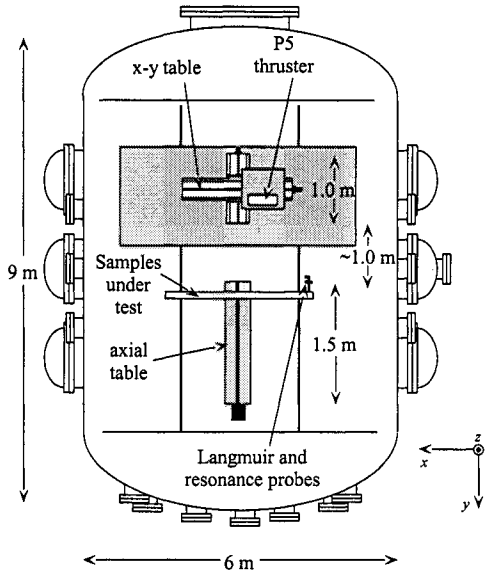

FIGURE 1. PEPL LVTF as Configured for Tests.

source. These tests were done, in part, to support design efforts for the follow-on mission to ProSEDS called STEP–Airseds, which will demonstrate multiple boost/deboost and inclination-change operations over a period of a year and covering from below 400-km to above 700-km altitude.

OML CURRENT COLLECTION

In the OML regime, the current, i, collected by a conductor in non-flowing plasma is given by the equation

$$i = n_e A_p q \frac{\sqrt{2}}{\pi} v_{te} \left(1 + \frac{qV_a}{kT_e}\right)^{0.5}. \tag{1}$$

The thermal velocity here is given by $v_{te} = \sqrt{kT_e/m_e}$. For high potentials ($V_a \gg kT_e/q$), Eqn. 1 reduces to

$$i = n_e A_p q \frac{\sqrt{2}}{\pi} \left(\frac{qV_a}{m_e}\right)^{0.5}. \tag{2}$$

We see that for large potentials, the current collected is independent of electron temperature and scales as the square root of the potential.

EXPERIMENTAL SETUP

PEPL has as its centerpiece the Large Vacuum Test Facility (LVTF), a cylindrical, stainless-steel-clad tank that is 9 m long and 6 m in diameter (Gallimore et al., 1996). The facility has four nude cryopumps backed by two 2000 cfm (56,600 l/s) blowers and four 400 cfm (11,300 l/s) mechanical pumps. These pumps give the facility a combined pumping speed of 300,000 l/s on air and 140,000 l/s on xenon and provide the ability to reach a high vacuum ($\sim 10^{-7}$ torr). Fig. 1 is a diagram of the LVTF as it was set up for these tests.

Two positioning tables were used to change the separation distance between the thruster and sample plane and to locate the sample under test (SUT) directly along the thruster's centerline. The thruster was mounted on an x–y table that could move axially 1.0 m and radially sufficient to cover all samples. The samples were mounted on an aluminum frame that was connected to an axial table that could move 1.5 m axially (samples are described in more detail below). Combined table movement allowed thruster-sample separation distance to change from $\sim$ 1 m to $\sim$ 3 m. Changing separation distance was the primary mechanism for changing the plasma density seen at the sample plane.

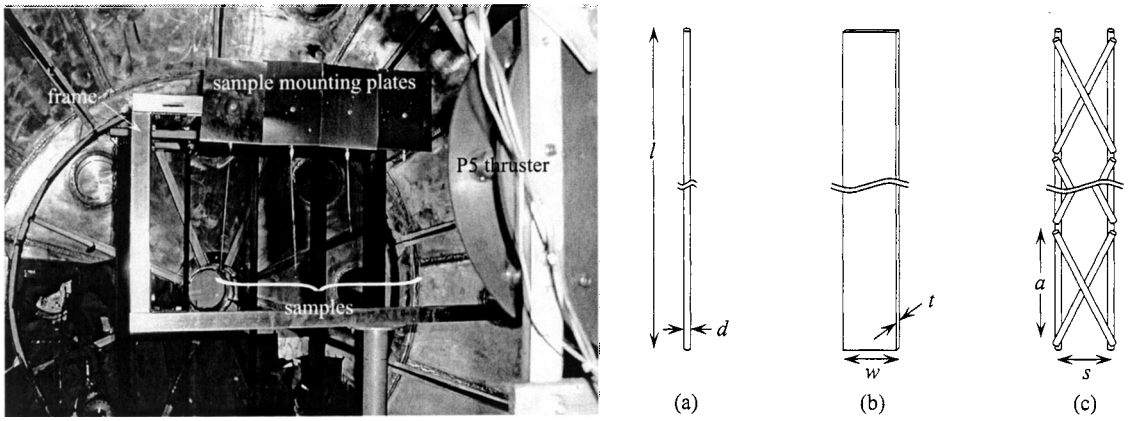

FIGURE 2. Picture of the Sample Support Structure for the Second Test Set; Structure for the First Test Set Was Very Similar. Schematics of Samples Used for Both Test Sets: (a) Reference Cylinder, (b) Flat Ribbon Tape, (c) Mesh.

Three different sample types were constructed for use during these tests: cylindrical, flat-ribbon tape, and sparse-ribbon or mesh. Only the cylindrical and flat ribbon results are discussed here. Tungsten metal was used for all samples to ensure that they would endure the expected high temperatures, which were caused by the collection of high-energy electrons to the samples' surfaces (Gilchrist et al., 2000). During the first set of tests, the samples were approximately 10 cm in length, whereas during the second set of tests, the samples were approximately 30 cm in length. Two tape samples were used in both test sets, one where the width dimension was perpendicular to the plasma flow, the other with the width dimension parallel to the plasma flow. The thickness of the tape was $t = 0.1$ mm. Sample dimensions were chosen so that they were on the order of 1–3 Debye lengths. Schematic representation of the samples is given in Fig. 2a–c. Sample descriptions are summarized in Table 1 and a more detailed sample description can be found in Gilchrist et al. (2000). A picture of the setup is also shown in Fig. 2.

TABLE 1. Descriptions of Samples Used for Both Test Sets.

	Sample	**1**	**2**	**3**	**4**	**5**
	Description	**Reference Cylinder**	**Perpendicular Tape**	**Parallel Tape**	**Perpendicular Mesh**	**Parallel Mesh**
first	length, l (cm)	10.0	9.4	9.2	9.8	9.5
test	Width, w, or	0.28	1.9 (top) to	2.0 (top) to	2.5 (top) to	2.5
set	Diameter, d (mm)		2.1 (bottom)	2.2 (bottom)	2.3 (bottom)	
second	length, l (cm)	29.5	29.5	29.5	27.6	n/a
test	Width, w, or	0.28	2.0 (top) to	2.0 (top) to	2.0 (top) to	n/a
set	Diameter, d (mm)		2.4 (bottom)	2.3 (bottom)	2.8 (bottom)	

The PEPL/AFRL "P5" 5-kW-class Hall-effect thruster was used to provide a flowing plasma for these experiments. A detailed description of the P5 is given by Haas et al. (1998). When operating nominally, the P5 plasma is much too dense for the conditions we needed; hence, for these tests the thruster was set at off-nominal conditions in order to lower the plasma density seen along the thruster's axial direction. The P5 operating conditions for both sets of tests are given in Table 2. For these experiments, the thruster was run on xenon propellant ($m_i = 2.18 \times 10^{-25}$ kg). An estimate for the average ion energy is that it lies in the range of $\sim$ 20–50 eV depending on losses that are not fully known at this time because the 100-V discharge voltage is below the nominal operating range for thruster operations. However, recent laboratory tests of other similar thrusters suggests this is a reasonable estimate.

We mention at this point several issues regarding the use of the P5 thruster as our plasma source. First, during these tests we did not have sensors available to help us resolve the flow character off axis from the P5. As the P5 is biased off nominal, this may become an issue. That is, the flow may be less directed than when the P5 operates nominally; however, this was partially compensated for by placing each sample in the same location with respect to the thruster

TABLE 2. Thruster Operating Parameters for Both Test Sets.

Parameter	First Test Set	Second Test Set
Chamber Pressure, Gauge 1 (torr)	1×10^{-5}	6.8×10^{-6}
Chamber Pressure, Gauge 2 (torr)	2×10^{-5}	1.5×10^{-5}
Discharge Voltage, V_d (V)	100	100
Discharge Current, I_d (A)	5.3	4
Inner Magnet Current, I_{im} (A)	2.99	1.04
Outer Magnet Current, I_{om} (A)	1.99	1.03
Cathode Voltage, V_c (V)	−19.7	−19.2
Heater Voltage, V_{htr} (V)	7.1	6.0
Anode Flowrate, $\dot{m}_a$ (sccm)	60	45
Cathode Flowrate, $\dot{m}_c$ (sccm)	6	6

at a given distance. Second, we were not able to measure the population of slow-moving ions. This also may become an issue because of the possibility for charge exchange between and accelerated ion and slow-moving neutrals. The P5 plasma environment as measured during these tests is presented below.

DATA

In order to better understand the data presented here, we present first the plasma environment for both test sets and then the data collected during those tests.

Plasma Environment

A detailed description of plasma diagnostics used is given in Gilchrist et al. (2000). Plasma measurements were taken using a Langmuir probe (LP) and resonance probe (RP) (Bilén et al., 1999). Fig. 3a reports the measured plasma environment as a function of distance for both test sets. By positioning the sample plane closer and farther from the thruster, we were able to obtain approximately a factor-of-10 change in plasma density. There are several qualifications that must be mentioned concerning the determination of the plasma environment. First, LP data were successfully gathered and analyzed for the first round of tests, but RP data were not collected. Unfortunately, during the second test set, the LP data could not be trusted. Hence, we utilized RP data for the 187-, 230-, and 305-cm positions. However, we had to estimate the 100-cm position from the OML current fits. Because the RP does not provide T_e measurements, we were unable to explicitly measure T_e for the second test set, but in comparison with data from the first test set, have set $T_e = 0.8$ eV for all positions. Having said this, we feel that we were able to provide a good description of the plasma environment for all tests.

Fig. 3b shows the calculated Debye lengths for both test sets. Debye length is given by the following equation

$$\lambda_D = \sqrt{\frac{\varepsilon_0 k T_e}{q^2 n_e}} \,. \tag{3}$$

The cylindrical sample had a radius $r = d/2 = 0.14$ mm, so we can see the Debye lengths obtained spanned a range of $\sim$ 1–3 times the cylinder's radius. The tape width of $\sim$ 2–2.4 mm represents from 5–16 times the Debye length.

Current Collection Data

This first set of figures (Figs. 4a–d) plots the current as a function of voltage for the tape and cylinder geometries from the second test set at separation distances of 305, 230, 187, and 100 cm, respectively, which represents lower to higher plasma density (see Fig. 3a). They also include the calculated OML currents to equal area equivalent cylinders (the tape equivalent cylinder radius is approximately 7 mm). As the separation distance is reduced, the effective width of the probes in terms of λ_D increases. In general, the calculated model response was near the experimental data. However, the data has important differences in features that will be discussed below. It is also noted that there is some difference between parallel and perpendicular tape orientations.

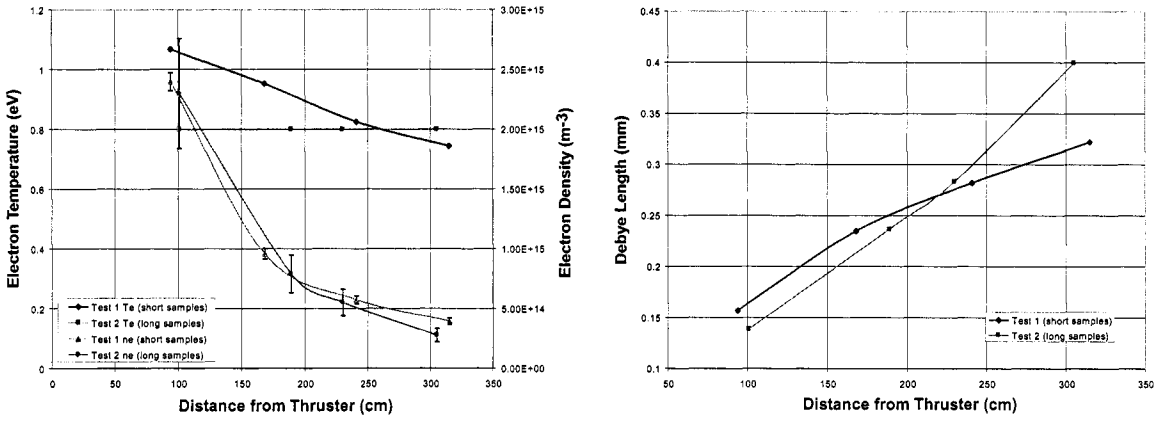

(a) (b)

FIGURE 3. (a) Plasma Parameters Measured for Both Test Sets. (b) Debye Lengths Derived for Both Test Sets.

Fig. 5 provides an example of differences between tests 1 and 2. To compare the differences between the two test runs, given the factor-of-three difference in sample length, the currents obtained in test 1 were multiplied by three before plotting. As seen in the figure, the cylinder samples were approximately the same, however, there is significant difference between the tape tethers. This is thought to be due to sample end-effects and is discussed below.

OBSERVATIONS AND ANALYSIS

There are several interesting and intriguing observations that result from the data collected during these tests and presented above. From Fig. 4 it can be seen that there is a small, but definite, difference between parallel and perpendicular orientations of the tape tether. In the figure it can be seen that the perpendicular orientation consistently exceeded the collected current of the parallel orientation and the difference appears to grow at higher densities (shorter Debye lengths). In all cases, collected currents are similar up to $\sim$ 50–70 V, at which point the collected current deviates for the two orientations. In all but the 100-cm case the difference in current for the orientations appears to reach a constant value that is maintained over the remaining potential range. The 100-cm case appears to show the two curves converging.

We can also interpret this separation between the parallel and perpendicular tape orientations in terms of a "knee" in the I–V curves that is particularly pronounced for the parallel tape case and is strongest at higher densities. We note that this knee occurs just above the estimated energy of the incoming beam of ions ($\sim$ 20–50 V). A separate knee is also evident at least for the 100-cm perpendicular tape case at a somewhat higher potential. At potentials below this knee, the current increases rapidly as potential is increased. Above the knee for the 305-, 230-, and 187-cm cases, the current increases at a rate more closely equivalent to OML current collection model. For the 100-cm case, the collected current appears to follow a shallower slope than predicted from OML theory.

We note that the presence of a difference in behavior at potentials below and above the incoming ion energy beam was seen in the TSS–1R (Thompson et al., 1998) and TSS–1 missions (Katz et al., 1993). In these situations, the presence of heating and turbulence could be detected in the plasma at bias potentials above the ion beam energy (Stone and Bonifazi, 1998). Additional measurements will be required to determine if similar effects are present for the tape samples here.

We find it also significant that an equal-area OML cylinder model closely agrees with the prediction of collected current as seen for the tape samples even though the width of the tape is much larger than a Debye length (see Fig. 4). Sanmartín and Estes (1999) considered tape geometries in the OML regime of a stationary, unmagnetized plasma and concluded that depending on potential and plasma temperature there are dimensions beyond a Debye where a thin tape could satisfy OML collection. Their conclusions for the case mosst appropriate to our experiments would suggest that the tape width could be up to four Debye lengths and still satisfy OML collection. Clearly, we have significantly exceeded this dimension here for our moving plasma. An upcoming paper by Estes and Sanmartín (2000) suggests

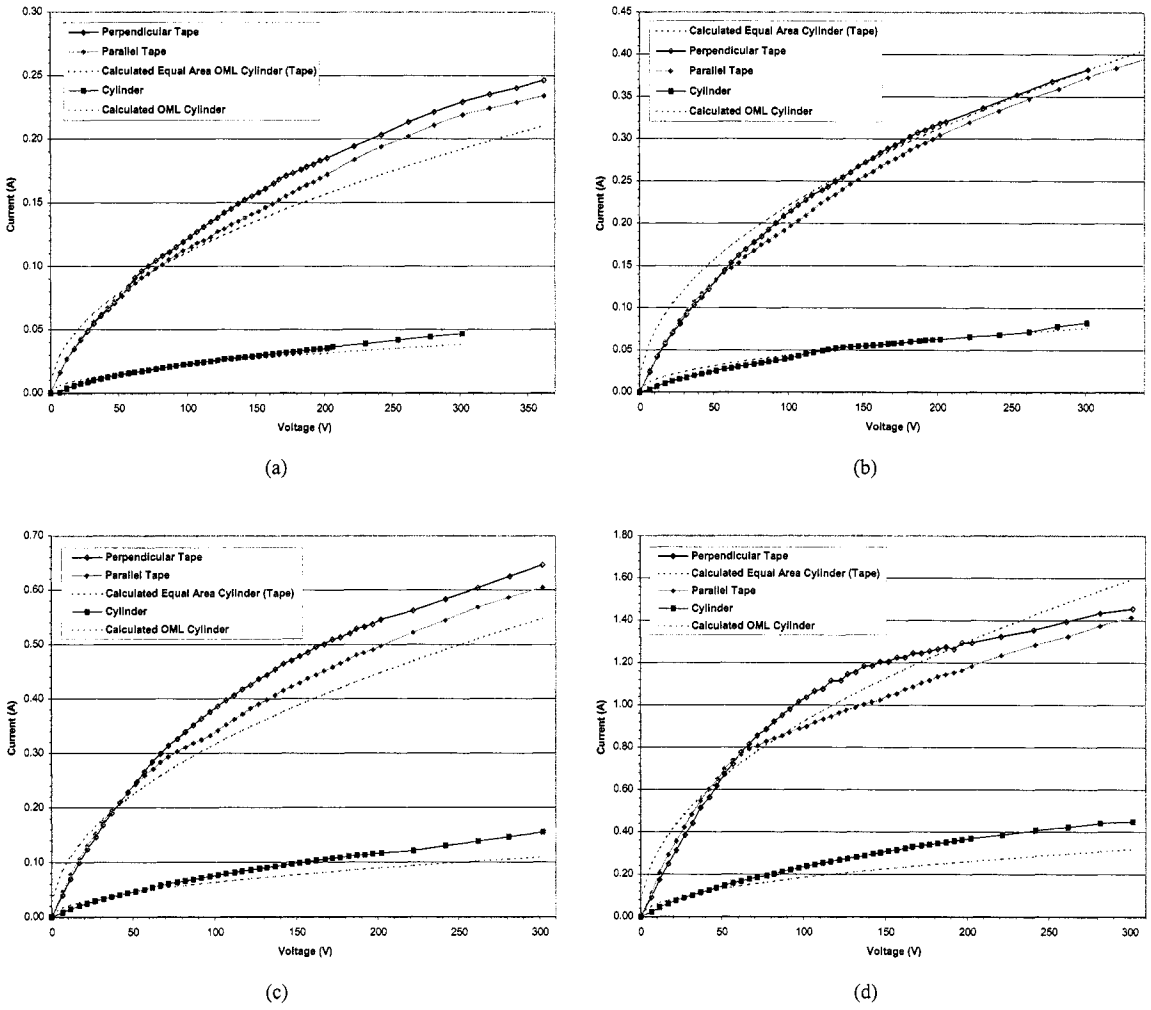

FIGURE 4. Current as a Function of Voltage for the Tape and Cylinder Geometries from the Second Test Set at Separation Distances of (a) 305 cm, (b) 230 cm, (c) 187 cm, and (d) 100 cm.

that their earlier threshold predictions are weak, *i.e.*, degradation in performance is not rapid beyond the theoretical limits. This certainly seems to be the case here. Further, the response at 100 cm where the tape is $\sim 15\lambda_D$ wide and where the current appears to be following a shallower slope may be indicative of exceeding the OML limit. Again, additional experiments will be required to answer this more clearly.

Fig. 5 compares our first and second test runs for the tape and cylinder cases at 94 and 100 cm. Here, the test-1 current has been multiplied by three to crudely compensate for the fact that the samples were three times shorter than the test-2 case. We attribute the difference in the tape results as being due to an end-effect even though the test-1 samples were over $600\lambda_D$ long (end-effects are also multiplied by this same factor of three). In fact, a major reason why the test-2 run was undertaken was to lengthen the probe samples such that it more completely covered the P5 plume region to minimize end effects. End effects are well known and they are often modeled by an ideal cylinder with an ideal spherical collector at the end, but the effective radius of the spherical collector is found to much wider than probe radius (Johannig et al., 1985). It is interesting to note that the cylinder samples did not show as much end effect as seen in the tape samples, which suggests a geometry factor must also be considered. In future experiments, we plan to use appropriate guards at each sample end, although the mechanical complexity for these small probes is considerable.

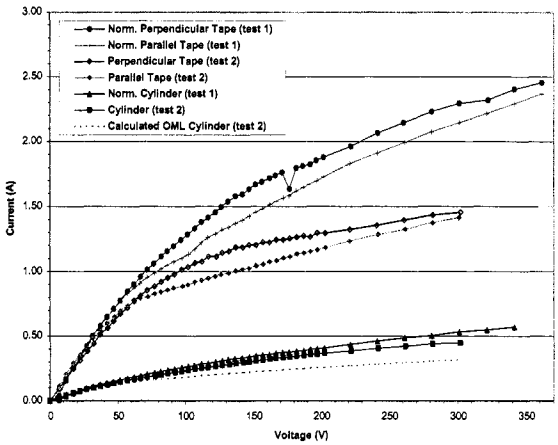

FIGURE 5. Comparison of Tests 1 and 2.

CONCLUSIONS

We believe the experimental results to date in high-speed plasma indicate that the tape tether will be a viable option for bare-tether geometries. Widths well above a Debye length can be used, but we are not able to say yet if there is an experimentally determined maximum dimension (*e.g.*, Sanmartín and Estes (1999)).

The tape sample current collection appears to generally agree with equal-area cylinder OML model. However, there is definitely non-OML character also present in the data, especially for the 100-cm case. Knees in the data appear just above the estimated ion beam energy range in all cases for the parallel orientation and the perpendicular case at the closest dimensions. It is also possible that at closest dimensions (100 cm), experimental data is not able to track OML theory at potentials starting around 5 times the ion beam energy (*i.e.*, 200 V). The differences between parallel and perpendicular orientation is also an example of high speed flow effect.

The possibility of end-effects even for our longer samples (test 2) does place some question on the overall quantitative assessment of the level of enhancement. In future experiments, a more sophisticated configuration can be used to minimize/eliminate this factor. However, we parenthetically note that adding an end collector may well be a positive enhancement for any bare EDT as our data suggests and suggested by others (Dobrowolny and Vannaroni, 1999).

We are planning future experiments to help clarify and expand upon these initial results. First, we will be including a guard to mitigate against end-effects in all samples. We plan on more fully mapping and characterizing the plume and its energy distribution. We will be increasing the effective width of the tape samples to approximately $30\lambda_D$. The mesh samples will be manufactured by cutting small holes through a solid tape sample. The density and geometry of these holes will be varied. Finally, we hope to be able to determine if turbulent effects are present in the near plasma as the bias is increased beyond the incoming ion beam energy. Different beam energies will also be used. Magnetic field effects may also be tested but this will require considerable effort for ground-based chamber tests.

NOMENCLATURE

a	mesh cross-member spacing, m
A_p	probe surface area, m^2
d	wire diameter, m
i	current, A
k	Boltzmann's constant, 1.38×10^{-23} J/K
l	tape length, m
m_e	electron mass, 9.109×10^{-31} kg
m_i	ion mass, kg
n_e	electron plasma density, m^{-3}
q	charge magnitude, 1.602×10^{-19} C
r	wire radius, m

s mesh cylinder spacing, m
t tape thickness, m
T_e electron temperature, K
V_a accelerating potential, V
v_{te} electron thermal velocity, m/s
w tape width, m
ε_0 free space permittivity, 8.85×10^{-12} F/m
λ_D Debye length, m

ACKNOWLEDGMENTS

The authors would like to thank the PEPL research group for assistance in performing these experiments. The authors thank Drs. R. Estes, N. Stone, and K. Wright for useful discussions about these results and their interpretation. This work was performed under contract from The Michigan Technic Corporation and NASA–MSFC.

REFERENCES

Bilén, S. G., Haas, J. M., Gulczinski III, F. S., Gallimore, A. D., and Letoutchaia, J. N., "Resonance-Probe Measurements of Plasma Densities in Electric-Propulsion Plumes," AIAA Paper AIAA–99–2714, 1999.

Dobrowolny, M., and Vannaroni, F., private communication, 1999.

Estes, R. D., and Sanmartín, J. R., "Cylindrical Langmuir Probes Beyond the Orbital-Motion-Limited Regime," submitted to *Physics of Plasmas*, (2000).

Forward, R. L., "Failsafe Multistrand Tether Structures for Space Propulsion," AIAA Paper AIAA–92–3214, 1992.

Gallimore, A. D., Kim, S.-W., Foster, J. E., King, L. B., and Gulczinski III, F. S., "Near and Far Field Plume Studies of a One-Kilowatt Arcjet," *AIAA J. Prop. Power* **12**, 105–111 (1996).

Gilchrist, B.E., Bilén, S. G., Patrick, T. A., and Van Noord, J. L., "Bare electrodynamic tether ground simulations in a dense, high-speed plasma flow," AIAA Paper AIAA–2000–3869, 2000.

Haas, J. M., Gulczinski III, F. S., Gallimore, A. D., Spanjers, G. G., and Spores, R. A., "Performance Characteristics of a 5 kW Laboratory Hall Thruster," *AIAA Paper AIAA–98–3503*, 1998.

Johannig, D., Seifert, W., and Best, A. "Analytic Density Correction for Cylindrical Langmuir Probes Showing End Effects, *Plasma Physics and Controlled Fusion* **27**, 159–179 (1985).

Johnson, L., Gilchrist, B. E., Estes, R. D., Lorenzini, E., and Ballance, J., "Propulsive Small Expendable Deployer System (ProSEDS) Space Experiment," AIAA Paper AIAA–98–4035, 1998.

Katz, I., Melchioni, E., Mandell, M., Oberhardt, M., Thompson, D., Neubert, T., Gilchrist, B., and Bonifazi, C., "Observations of Ionosphere Heating in the TSS–1 Subsatellite Presheath," *J. Geophysical Research* **99**, 8961–8969 (1993).

Sanmartín, J. R., Martinez-Sánchez, M., and Ahedo, E., "Bare Wire Anodes for Electrodynamic Tethers," *J. of Prop. and Power* **9**, 353–360 (1993).

Sanmartín, J. R., and Estes, R. D., "The Orbital-Motion-Limited Regime of Cylindrical Langmuir Probes," *Physics of Plasmas* **6**, 395–405 (1999).

Stone, N. H., and Bonifazi, C., "The TSS–1R Mission: Overview and Scientific Context," *Geophysical Research Letters* **25**, 409–412 (and papers therin) (1998).

Thompson, D. C., Bonifazi, C., Gilchrist, B. E., Williams, S. D., Raitt, W. J., Lebreton, J.–P., Burke, W. J., Stone, N. H., and Wright, Jr., K. H., "The Current–Voltage Characteristics of a Large Probe in low Earth Orbit: TSS–1R Results," *Geophysical Research Letters* **25**, 413–416 (1998).